High pressure computational search of trivalent lanthanide di-nitrides

High pressure computational search of trivalent lanthanide di-nitrides

Francesca Menescardi,[†] Emma Ehrenreich-Petersen,[¶] and Davide Ceresoli[*,‡]

†*Dipartimento di Chimica, Università degli Studi di Milano, via Golgi 19, 20133 Milan, Italy*

‡*Consiglio Nazionale delle Ricerche, Istituto di Scienze e Tecnologie Chimiche (CNR-SCITEC), via Golgi 19, 20133 Milan, Italy*

¶*Department of Chemistry and iNANO, Aarhus University, Langelandsgade 140, 8000 Aarhus C, Denmark*

E-mail: davide.ceresoli@cnr.it

Abstract

Transition metal nitrides have attracted much interest of the scientific community for their intriguing properties and technological applications. Here we focus on yttrium dinitride (YN_2) and its formation and structural transition under pressure. We employed a fixed composition USPEX search to find the most stable polymorphs. We choose yttrium as a proxy for the lanthanide series because it has only +3 oxidation state, contrary to most transition metals. We then computed thermodynamic and dynamical stability of these structures compared to the decomposition reactions and we found that the compound undergoes two structural transitions, the latter showing the formation N_4 chains. A closer look into the nature of the nitrogen bonding showed that in the first two structures, where nitrogen forms dimers, the bond length is intermediate between that of a single bond and that of a double bond, making it hard to rationalize the proper oxidation state configuration for YN_2. In the latter structure

where there is the formation of N_4 chains, the bond lengths increase significantly, up to a value that can be justified as a single bond. Finally, we also studied the electronic structure and the dynamical stability of the structures we found.

1 Introduction

The intriguing properties and potential vast application of transition metal nitrides (TMNs) have attracted the interest of the scientific community in recent years.[1–7] In general, nitrides are much less studied than the corresponding oxygen-based compounds, but have been shown to give rise to ultrahard[8–14] and superconducting[15,16] materials that can find application in modern technologies as field effect transistors, p-n junctions and energy storage devices.[6,7]

In this work we focus on binary nitrides with a formally trivalent cation, such as a rare-earth ion. Nitrogen-rich compounds that can be synthesized under high pressure, exhibit intriguing properties compared to the mononitrides. In fact, besides the excellent mechanical properties that arise, when $M-N_x$ compounds are synthesized under pressure, they tend to form fairly long chains of nitrogen atoms. The consequent formation of high energy, single $N-N$ bonds is an effective way to store chemical energy.[1] This is not surprising as nitrogen itself is know to polymerize at 110 GPa and 2000 K, forming the so called *cubic gauche* structure. Very recently, a new polymeric polymorph resembling black phosphorous was synthetized.[17] Moreover, it is known that the alloying of nitrogen with alkali or with transition metal ions is an effective way to decrease the polymerization pressure.[3]

The mononitrides with a trivalent rare-earth cation are reported to form simple packed structures under pressure (B1, B2, B10)[18–20] with a suggested formal oxidation state configuration $M^{3+}N^{3-}$, resulting in small to wide band-gap semiconductors.[21] On the contrary, several valence configurations have been proposed[22] to explain the nature of the nitrogen chemical bonding and its relation to the physical properties of MN_2 materials. Tetravalent cations form compounds with formal oxidation $M^{4+}(N_2)^{4-}$ that are called *pernitrides* and are characterized by a $N-N$ bond length of $\sim$1.42 Å. Divalent cations form compound

with formal oxidation state $M^{2+}(N_2)^{2-}$ that are called *dinitrides* and display a significantly shorter N=N bond length of about 1.23 Å. The case of a trivalent rare-earth cation does not seem to fit in any of the two definitions, and the understanding of the nature of N..N bond in this case is not so intuitive. In a recent work, Wessel et al.[22] rationalized the nature of the nitrogen bonding in LaN_2 compound, suggesting a possible mechanism for the formation of this non-trivial structure. Indeed, forcing the N_2 moiety away from the -2 and -4 oxidation states, could be an effective way towards the formation of long nitrogen chains.

To explore these concepts we studied the structural, electronic and formation properties of yttrium dinitride (YN_2) under pressure. We choose yttrium as a proxy for lanthanides, because it is always trivalent, avoiding the multiple valence character of some lanthanides ions. Moreover, from a computational point of view, yttrium displays empty highly-localized $4f$ orbitals, thus avoiding complications such as magnetism and strong correlation, that arise when in presence of partially filled f orbitals.

We applied an ab-initio crystals structure prediction (CSP) method[23] to search for the most stable YN_2 polymorphs up to 100 GPa. We computed the thermodynamic and dynamic stability of the obtained polymorphs down to ambient pressure and with respect to the decomposition reaction $YN_2 \rightarrow YN + \frac{1}{2}N_2$. Finally we compared the nitrogen bond length and bulk modulus to a set of existing compounds and in order to rationalize the nature of chemical bonds and to understand which formal valence better describes the chemistry of these compounds.

2 Computational methods

We performed a fixed composition USPEX (v9.4.4) search on four YN_2 unit formula. The initial USPEX population was composed of 40 randomly generated structures and we allowed up to 25 generations, employing the standard genetic algorithms (heredity, random generation, soft mutation, permutation and lattice mutation).[24–26] The external pressure was set

to 100 GPa, about double the highest pressure that is expected to lead to the experimental synthesis of pernitrides. To reduce the computational cost, we used the local-basis code SIESTA,[27] with norm-conserving pseudopotentials from the Martins-Trouiller table and the SZP basis set with a 50 meV energy shift. The mesh cutoff was 250 Ry. We used the PBE exchange correlation functional.[28]

At the end of the USPEX run, we selected the 20 most stable structures, after pruning those we found equivalent by symmetry. These structures were further relaxed down to ambient pressure in steps of 10 GPa with the plane-wave pseudopotential code Quantum Espresso.[29,30] We used the PBE functional, ultra-soft pseudopotentials from the GBRV library,[31] wave function/density cutoffs of 45/450 Ry and up to 6×6×6 k-points. The electronic density of states was computed on a finer k-point mesh. The phonon density of states were computed using the density functional perturbation theory (DFPT) method[32] with a density cutoff of 900 Ry.

3 Results

3.1 YN_2 structures

Within the maximum pressure range of 100 GPa, we found three stable polymorphs among all the structures produced by USPEX (Fig. 1). The other higher energy polymorphs, not reported in this paper, usually differ from the the most stable one, by the stacking of the layers. We note that even though the polymorphs appear like layered structures, the interlayer interaction is not van der Waals or dispersion. Hence, the layer stacking has a strong impact on the enthalpy of the system.

At ambient pressure, we predict that YN_2 will adopt the ThC_2 (space group $C2/c$[33]) crystal structure (Fig. 2a), characterized by alternating layers of Y and N_2 dimers. Upon increasing the pressure the structure undergoes a structural phase transition at GPa into a more compact $P2_1/c\#1$ structure (Fig. 2b), still with N_2 dimers, but with no evident

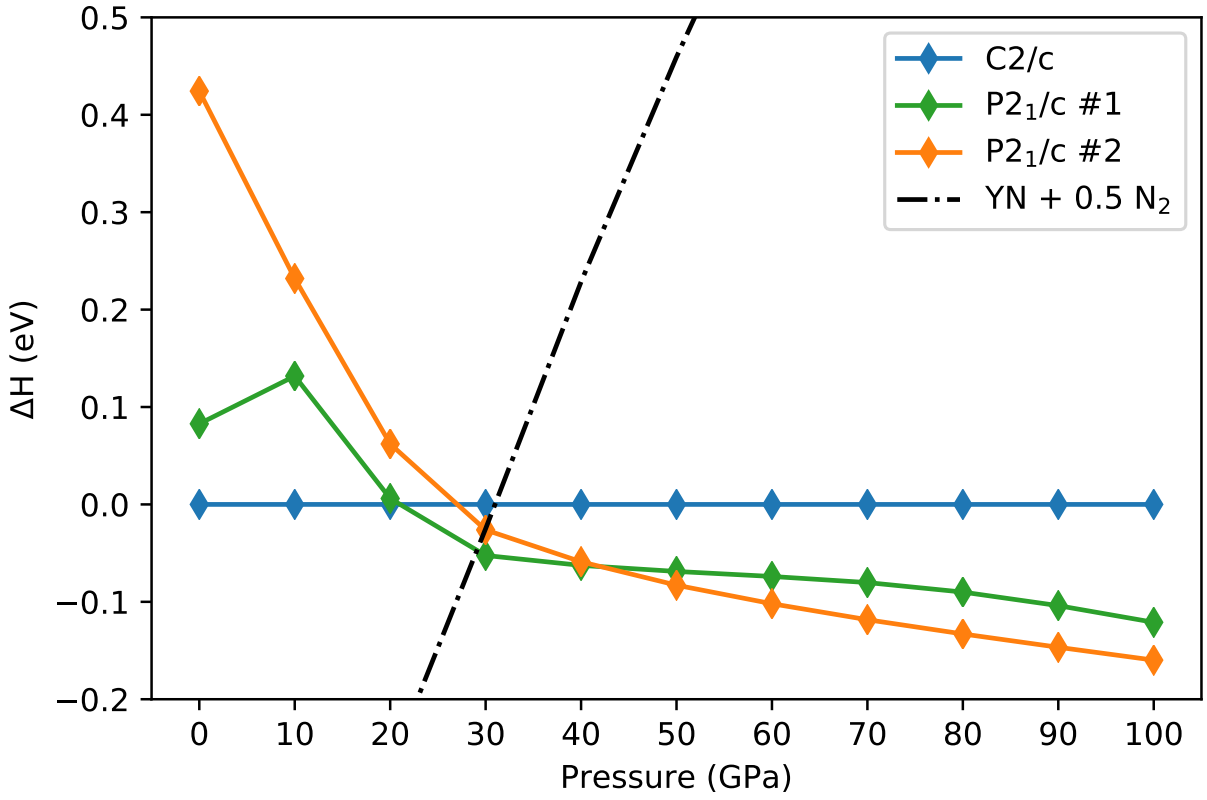

Figure 1: Calculated enthalpy as function of pressure, of the three most stable YN_2 polymorphs, relative to the enthalpy of the ThC_2 structure. The dashed line marks the enthalpy of bulk YN (B1 structure) plus $\frac{1}{2}N_2$ (ϵ-N_2 structure).

alternate layers of Y and N_2. Then, at 40 GPa, it turns into another monoclinic structure with the same symmetry ($P2_1/c\#2$), but with by N_4 moieties (Fig. 2c). The N_4 chains persist up to the highest investigated pressure of 100 GPa. The lattice parameters and the Wyckoff positions of the structures at 0, 30, 50 and 100 GPa are listed in Tab. 1.

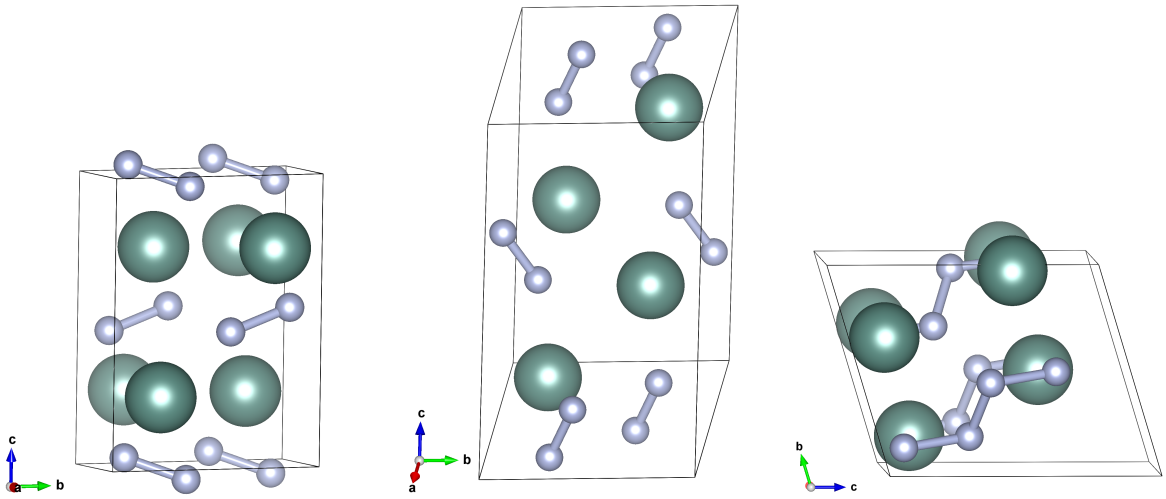

(a) (b) (c)

Figure 2: Fully optimized YN_2 structures. (a) C2/c (ThC_2) structure at 0 GPa. (b) $P2_1/c\#1$ structure at 30 GPa. (c) $P2_1/c\#2$ structure at 50 GPa. The green spheres are the Y ions, the small gray spheres are the N ions.

Fig. 3 shows the volume of the structures considered in this work. Here, volume is seen to decrease as a consequence of the great pressure applied. In addition, a noticeable volume drop is seen for both the first structural transition (20 GPa, 3.25%) and the second structural transition (40 GPa, 1.07%). Clearly, the volume drop of the second transition is lower and both structural transitions are probably of first-order.

In Fig. 1 we also report the enthalpy of bulk YN (B1 structure) + $\frac{1}{2}N_2$. The USPEX search on the mononitride YN found that the B1 structure is by far the most stable polymorph in the pressure range. For sake of simplicity, we took the $\epsilon-N_2$ polymorph to model solid nitrogen in the whole pressure range as it is reported to be the most stable polymorph between 13 GPa and 69 GPa. We found that in this pressure range, below 30 GPa the $P2_1/c\#1$ is not thermodynamically stable and it decomposes into YN and N_2.

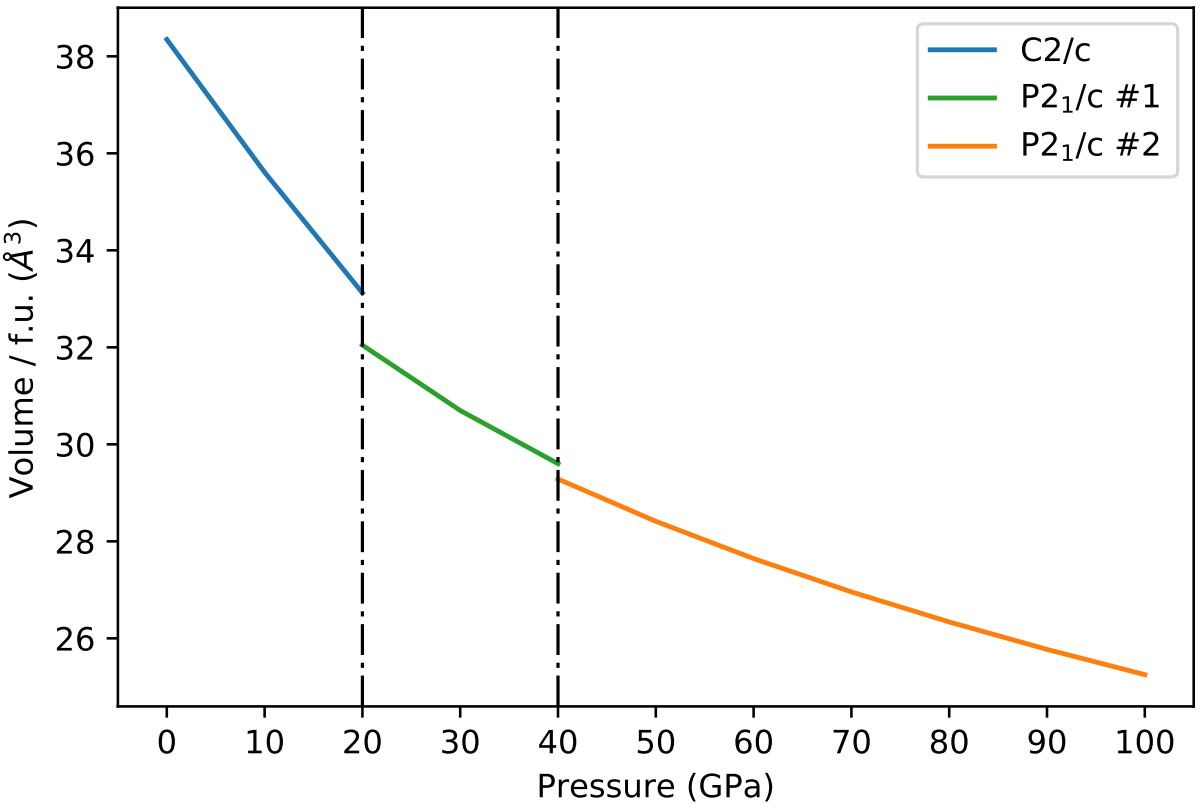

Figure 3: Calculated volume per formula unit as function of pressure. The vertical lines indicate the transition pressures.

Table 1: Lattice parameters, space group and Wyckoff positions of the YN_2 structures, at selected pressures.

Phase	Pressure	Lattice	Sites	Coordinates
C2/c	0 GPa	a=6.0492 Å	4e	Y: 0.0000, 0.2276, 0.2500
(s.g. 15)		b=4.2245 Å	8f	N: 0.2260, 0.5389, 0.5389
		c=6.2247 Å		
		β =74.64°		
$P2_1/c$#1	30 GPa	a=4.3842 Å	4e	Y: 0.6205, 0.7824, 0.9175
(s.g. 14)		b=4.7349 Å	4e	N: 0.0289, 0.9216, 0.3154
		c=7.7441 Å	4e	N: 0.7500, 0.2130, 0.4771
		β =134.50°		
$P2_1/c$#2	50 GPa	a=5.6303 Å	4e	Y: 0.7723, 0.0131, 0.1563
(s.g. 14)		b=4.6147 Å	4e	N: 0.8210, 0.5166, 0.1802
		c=4.5694 Å	4e	N: 0.4336, 0.0820, 0.3679
		β =108.80°		
$P2_1/c$#2	100 GPa	a=5.4306 Å	4e	Y: 0.7695, 0.0232, 0.1518
(s.g. 14)		b=4.4185 Å	4e	N: 0.8262, 0.5283, 0.1761
		c=4.3994 Å	4e	N: 0.4333, 0.0844, 0.3666
		β =106.90°		

We also run a USPEX calculation with three unit formula but the structures obtained are less thermodynamically stable than the structures with four unit formula. The reason is that the former are characterized by a N_2 and a N_4 moiety. These "4+2" structures could be considered as intermediate between the $P2_1/c$ #2 and the $P2_1/c$ #1, where the N_4 chains break into pairs of N_2 molecules as the pressure is lowered. Interestingly, we didn't find nor any N_3 moiety neither cyclic nitrogen species stable enough to be competitive with the structures reported so far.

3.2 Dynamical stability

To establish that the predicted structures are dynamically stable, we calculated the phonon dispersion on a q-point mesh of 3×3×3. In Fig. 4 we report just the phonon density of states, rather than the phonon dispersion since all structures are monoclinic. From Fig. 4 we found that the ThC_2-structure is dynamically unstable at ambient pressure. Inspection of the unstable phonon modes, reveals that the stable structure would display a long wave-

length modulation of the relative distance between the Y and N_2 sublattices. However, the $P2_1/c\#1$ structure is thermodynamically unstable against the decomposition, as shown previously. Therefore, this lattice modulation, akin to a charge density wave instability would be extremely difficult to observe in experiments. On the contrary, the other two structures are dynamically stable since all the phonon frequencies are real and positive. An interesting feature is that the nitrogen contributes mainly to the high energy optical modes at frequencies 1000 cm^{-1} and above. In the low energy region, there is still a noticeable separation between Y and N vibrations. Indeed the heavy Y ion contributes mainly to the lowest energy phonon (below 200 cm^{-1}), whereas the intermediate energy region is largely characterized by vibrational modes involving nitrogen only.

3.3 Electronic structure and chemical bonding

In Fig. 5 we report the projected electronic density of states of selected structures, with respect to the Fermi level. The C2/c (0 GPa) and $P2_1/c\#1$ (30 GPa) structures are metallic and their valence band has a large N $2p$ character. The Y states instead contribute mainly to the empty states. From the electronic structure point of view the formal valence of these polymorphs is closer to $Y^{+2}(N_2)^{2-}$ rather than to $Y^{+4}(N_2)^{4-}$, i.e. closer to the *dinitride* structure. The presence of a unique N..N bond length indicates that bond disproportionation (i.e. $(Y^{3+})_2(N_2)^{2-}(N_2)^{4-}$) does not takes place. This is conceivable since the electronic screening of the metallic state tends to delocalize the charge carriers and suppresses the ionic character.

The situation changes upon increasing the pressure above 50 GPa, following the formation of the N_4 moieties. The electronic density of states is semimetallic, with a low density of states up to $\sim$2 eV above the Fermi level. This can be explained by the formal valence $(Y^{3+})_2(N_4)^{6-}$, in which the N_4 moiety has 6 extra electrons (i.e. 26 valence electrons). The 26 valence electrons (13 electron pairs) could be naively arranged as 3 single bonds and 10 lone pairs as shown by the Lewis structure with single N$-$N bonds as shown in Fig. 6.

(a)

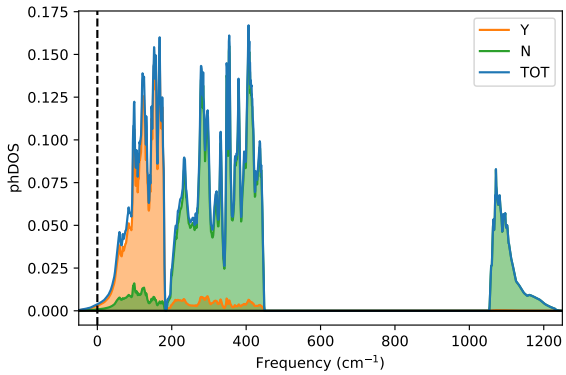

(b)

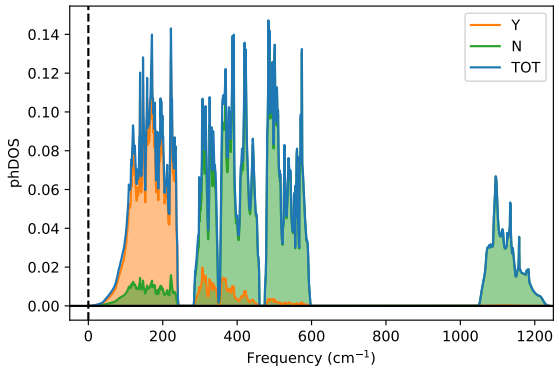

(c)

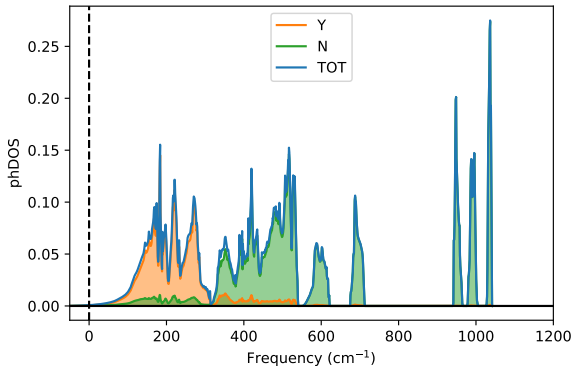

Figure 4: Calculated phonon density of states of the thermodynamically stable structures. (a) C2/c phase at 0 GPa; (b) $P2_1/c$#1 phase at 30 GPa; (c) $P2_1/c$#2 phase at 50 GPa. The Y and N contributions to the phonon density of states are indicated by the orange and green shaded areas, respectively.

Moreover, the $(N_4)^{6-}$ moiety fulfills the $6n+2$ Wade rule in n-member linear chains. However the Lewis structure does not reflect the actual charge distribution and chemical bonding. In fact the $(N_4)^{6-}$ anion is planar, indicating a partial multi-center π bonding. In principle this structure would possess a finite band gap, but the increased overlap due to the external pressure tends to close the gap. Notice also the increase of the band width of the occupied states and the larger hybridization between Y and N states. Whereas the low pressure phases can be described as intermetallic, the high pressure phase could be described more as a salt-like, Zintl phase. This hypothesis could be confirmed or disproved by advanced chemical bond analysis.[34,35] Interestingly, a $(N_4)^{6-}$ anion in the planar *cis* conformation is found in the USPEX search but its enthalpy is larger than that of the *trans* conformation.

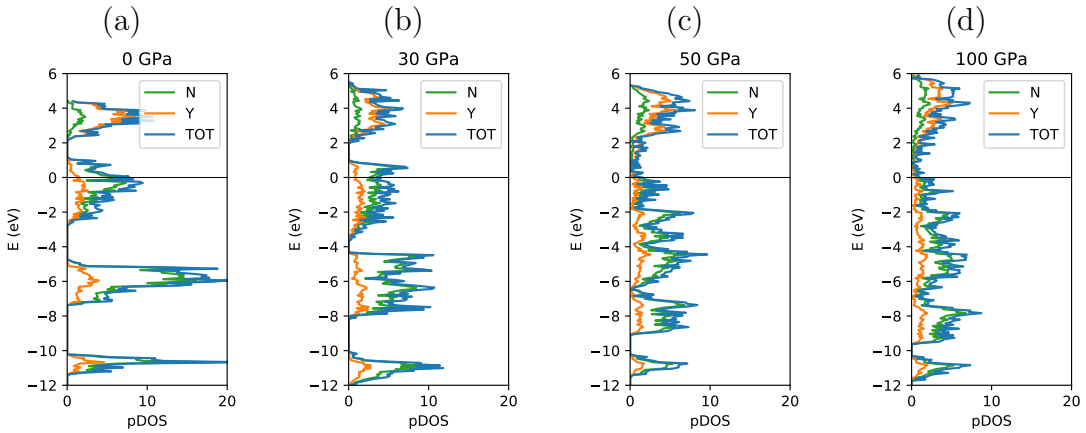

Figure 5: Projected electronic density of states of selected polymorphs and pressure. (a) C2/c at 0 GPa. (b) $P2_1/c$#1 at 30 GPa. (c) and (d) $P2_1/c$#2 at 50 and 100 GPa. The Fermi level is denoted by the black horizontal line.

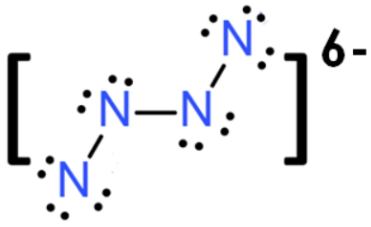

Figure 6: The simplest Lewis structure with only σ bonds of the $(N_4)^{6-}$ moiety found in the $P2_1/c$#2 structure. In reality the chemical bonding has a partial multicenter π contribution.

4 Discussion

It is interesting to study the behavior of N..N bond length as a function of pressure and compare to other di-nitrides. The ThC_2-like structure at ambient pressure has a N..N bond length of 1.33 Å, which is intermediate between a single and a double bond (see Tab. 2). Indeed, when the cation is divalent (like in the dinitrides as BaN_2), N_2 is better described in the form $(N{=}N)^{2-}$, whereas if the cation valence is higher (like in the pernitrides as PtN_2), the N_2 moiety is best described as $(N{-}N)^{4-}$. In this particular case, however, the situation is more challenging to rationalize, since there is no evidence of the yttrium cation being either divalent or tetravalent: it is always reported as trivalent. This consideration brings us to consider two different options to rationalize the valence of these compounds: the first possibility is to have static fluctuations in the N_2 bond lengths, where some N..N longer bonds are longer than others averaging out to around 1.33 Å; the second possibility is to have an electron forming a partially filled band. The analysis of the DOS in Fig. 5 seems to suggest the second scenario. This has been already proposed to be the case of LaN_2.[22] After the first structural transition, the situation remains similar, with a $N{-}N$ bond length of 1.32 Å.

Table 2: Nitrogen-nitrogen bond lengths in various pernitrides and dinitrides, reported from literature as well as calculated in the present work for YN_2, as a function of pressure.

Structure	$N{-}N$ bond length / Å	Ref.
BaN_2	1.23	Ref.[22]
PtN_2	1.41	Ref.[22]
OsN_2	1.43	Ref.[11]
IrN_2	1.30	Ref.[36]
LaN_2	1.30	Ref.[22]
YN_2, C2/c, 0 GPa	1.33	this work
YN_2, $P2_1/c$#1, 30 GPa	1.32	present work
YN_2, $P2_1/c$#2, 50 GPa	1.42, 1.44	present work
YN_2, $P2_1/c$#2, 50 GPa	1.39, 1.40	present work

The situation changes dramatically after the second transition, at 40 GPa, with the formation of N_4 chains, the bond lengths increase significantly with respect to lower pressures:

the central bond is 1.42 Å and the two others are 1.44 Å. Indeed, the $(N_4)^{6-}$ moiety can be described by a single Lewis formula with all single N−N bonds. As a consequence, the system is a closed shell and the solid is semimetallic. At the very high pressure of 100 GPa the N-N bond lengths in N_4 moiety become 1.39 and 1.40 Å.

Wessel and collaborators[22] observed that mechanical hardness and bulk modulus are larger in pernitrides than in dinitrides, due to the different character and filling of N_2 orbitals. We calculated the bulk modulus of the three YN_2 polymorphs by fitting to the Birch-Murnaghan 3rd order equation of state.[37] The results are reported in Tab. 3, and compared to other dinitrides and pernitrides from literature. Indeed, the low pressure YN_2 phases display a bulk modulus larger than the dinitride BaN_2 and similar to that of LaN_2. Interestingly, upon the formation of N_4 chains, the bulk modulus increases by ∼60 GPa.

Table 3: Bulk moduli in various pernitrides and dinitrides, reported from literature as well as calculated in the present work for YN_2 with EosFit[39] (Birch-Murnaghan, 3rd Order).

Structure	Bulk Modulus (GPa)	Ref.
BaN_2	46	Ref.[9]
SrN_2	65	Ref.[9]
PtN_2	256	Ref.[9]
OsN_2	358	Ref.[36]
IrN_2	428	Ref.[38]
LaN_2	86	Ref.[9]
YN_2, C2/c	117	present work
YN_2, $P2_1/c$#1	118	present work
YN_2, $P2_1/c$#2	174	present work

Regarding superconductivity one could estimate estimate T_c from the BCS formula $T_c = 1.134\, T_D \exp\left[1/(N_0\, g)\right]$ which links the superconducting temperature to the Debye temperature T_D (which is high in hard materials), to the density of states at the Fermi level N_0 and to the average electron phonon coupling g. Our dinitrides are not super-hard materials compared to transition metal mono-nitrides.[15,16] There is no particular reason to expect a large electron phonon coupling and the density of states at the Fermi level is not very large. As a consequence, we expect that YN_2 T_c to be smaller than that of the mono-nitrides and much smaller that the superconducting hydrides.[40]

Our methods can be applied to study the formation and stability of the series of LnN_2 compounds (Ln=La..Lu). We expect that as the size of the cation is reduced the phase transition will occur at higher pressure and new compact structures might be found. Lanthanide cations with multiple oxidation states (i.e. Ce, Pr, Sm, Eu, Tb, Tm, Yb) will represent a challenge for DFT and one must employ advanced techniques like dynamical mean field theory (DMFT).[41]

5 Conclusions

We found by crystal structure prediction the most stable structures of YN_2 up to 100 GPa. At low pressure, the system adopts the ThC_2 structure like LaN_2. Unfortunately this structure is thermodynamically unstable with respect to the decomposition into YN and solid N_2 and dynamically unstable at ambient pressure. This structure is characterized by N_2 dimers and, upon increasing pressure, it transforms into a monoclinic polymorph ($P2_1/1\#1$) with no evident N_2 layers. By comparing the nitrogen bond length and the bulk modulus, we arrive at the conclusion that both C2/c and $P2_1/1\#1$ predicted polymorphs can be categorized as *dinitrides* and the N_2 chemical bond is closer to a double N=N bond. Finally, above 40 GPa, N_4 moieties are formed and the structure is semimetallic. We verified the dynamical stability of the two high pressure structures by computing the phonon density of states. Our work is the first step towards studying the formation and stability of LnN_2 compounds (Ln=La..Lu). In principle we can substitute Y with any lanthanide in every structure generated my USPEX and compute the enthalpies in the whole pressure range. This will provide a tentative phase diagram for each LnN_2 compound that will provide useful indication for future high pressure experiments.

Acknowledgement

We acknowledge financial support from the Center for Materials Crystallgraphy (CMC). We thank Martin Bremholm and Carlo Gatti for helpful discussions. Calculations were performed at the CINECA supercomputing center thanks to the ISCRA HP10C7BPGD, HP10C5WGQ7 and HP10CPXESJ grants.

References

(1) Steele, B. A.; Stavrous, E.; Prakapenka, V. B.; Radousky, H.; Zaug, J.; Crowhurst, J. C.; Oleynik, I. I. Cesium pentazolate: A new nitrogen-rich energetic material. *AIP Conference Proceedings* **2017**, *1793*, 040016.

(2) Wu, L.; Tian, R.; Wan, B.; Liu, H.; Gong, N.; Chen, P.; Shen, T.; Yao, Y.; Gou, H.; Gao, F. Prediction of Stable Iron Nitrides at Ambient and High Pressures with Progressive Formation of New Polynitrogen Species. *Chemistry of Materials* **2018**, *30*, 8476–8485.

(3) Xia, K.; Zheng, X.; Yuan, J.; Liu, C.; Gao, H.; Wu, Q.; Sun, J. Pressure-Stabilized High-Energy-Density Alkaline-Earth-Metal Pentazolate Salts. *The Journal of Physical Chemistry C* **2019**, *123*, 10205–10211.

(4) Jiao, F.; Zhang, C.; Xie, W. High-Pressure FeN_x: Stability, Phase Transition, and Energetic Characteristic. *The Journal of Physical Chemistry C* **2020**, *124*, 19953–19961.

(5) Wang, B.; Larhlimi, R.; Valencia, H.; Guégan, F.; Frapper, G. Prediction of Novel Tin Nitride Sn_xN_y Phases Under Pressure. *The Journal of Physical Chemistry C* **2020**, *124*, 8080–8093.

(6) Zhou, M.; Liu, S.; Du, M.; Shi, X.; Zhao, Z.; Guo, L.; Liu, B.; Liu, R.; Wang, P.;

Liu, B. High-Pressure-Induced Structural and Chemical Transformations in NaN_3. *The Journal of Physical Chemistry C* **2020**, *124*, 19904–19910.

(7) Zhou, M.; Sui, M.; Shi, X.; Zhao, Z.; Guo, L.; Liu, B.; Liu, R.; Wang, P.; Liu, B. Lithium Pentazolate Synthesized by Laser Heating-Compressed Lithium Azide and Nitrogen. *The Journal of Physical Chemistry C* **2020**, *124*, 11825–11830.

(8) Auffermann, G.; Prots, Y.; Kniep, R. SrN and SrN_2: Diazenides by synthesis under high N_2-pressure. *Angewandte Chemie - International Edition* **2001**, *40*, 547–549.

(9) Weihrich, R.; Eyert, V.; Matar, S. F. Structure and electronic properties of new model dinitride systems: A density-functional study of CN_2, SiN_2, and GeN_2. *Chemical Physics Letters* **2003**, *373*, 636–641.

(10) Weihrich, R.; Matar, S. F.; Betranhandy, E.; Eyert, V. A model study for the breaking of N_2 from CN_x within DFT. *Solid State Sciences* **2003**, *5*, 701–703.

(11) Wang, Z.-H.; Kuang, X.-Y.; Zhong, M.-M.; Lu, P.; Mao, A.-J.; Huang, X.-F. Pressure-induced structural transition of OsN_2 and effect of metallic bonding on its hardness. *EPL (Europhysics Letters)* **2011**, *95*, 66005.

(12) Bhadram, V. S.; Kim, D. Y.; Strobel, T. A. High-pressure synthesis and characterization of incompressible titanium pernitride. *Chemistry of Materials* **2016**, *28*, 1616–1620.

(13) Alkhaldi, H.; Kroll, P. Chemical Potential of Nitrogen at High Pressure and High Temperature: Application to Nitrogen and Nitrogen-Rich Phase Diagram Calculations. *The Journal of Physical Chemistry C* **2019**, *123*, 7054–7060.

(14) Pillai, S. B.; Soni, H. R.; Jha, P. K. First principles high pressure studies on group-14 element pernitrides. *Journal of Alloys and Compounds* **2020**, *819*, 153193.

(15) Shy, Y. M.; Toth, L. E.; Somasundaram, R. Superconducting properties, electrical

resistivities, and structure of NbN thin films. *Journal of Applied Physics* **1973**, *44*, 5539–5545.

(16) Wang, S.; Antonio, D.; Yu, X.; Zhang, J.; Cornelius, A. L.; He, D.; Zhao, Y. The Hardest Superconducting Metal Nitride. *Scientific Reports* **2015**, *5*.

(17) Laniel, D.; Winkler, B.; Fedotenko, T.; Pakhomova, A.; Chariton, S.; Milman, V.; Prakapenka, V.; Dubrovinsky, L.; Dubrovinskaia, N. High-Pressure Polymeric Nitrogen Allotrope with the Black Phosphorus Structure. *Phys. Rev. Lett.* **2020**, *124*, 216001.

(18) Yang, J.; Gao, F.; Wang, H.; Gou, H.; Hao, X.; Li, Z. Elastic properties and hardness calculations of lanthanide nitrides in rocksalt structure. *Materials Chemistry and Physics* **2010**, *119*, 499–504.

(19) Nielsen, M. B.; Ceresoli, D.; Jørgensen, J.-E.; Prescher, C.; Prakapenka, V. B.; Bremholm, M. Experimental evidence for pressure-induced first order transition in cerium nitride from B1 to B10 structure type. *Journal of Applied Physics* **2017**, *121*, 025903.

(20) Ehrenreich-Petersen, E.; Nielsen, M. B.; Bremholm, M. Experimental equation of state of 11 lanthanide nitrides (NdN to LuN) and pressure induced phase transitions in NdN, SmN, EuN, and GdN. *Journal of Applied Physics* **2020**, *128*, 135902.

(21) Tie-Yu, L.; Mei-Chun, H. Electronic structure of ScN and YN: density-functional theory LDA and GW approximation calculations. *Chinese Physics* **2006**, *16*, 62–66.

(22) Wessel, M.; Dronskowski, R. Nature of N-N bonding within high-pressure noble-metal pernitrides and the prediction of lanthanum pernitride. *Journal of the American Chemical Society* **2010**, *132*, 2421–2429.

(23) Oganov, A. R., Saleh, G., Kvashnin, A. G., Eds. *Computational Materials Discovery*; The Royal Society of Chemistry, 2019.

(24) Oganov, A. R. Crystal structure prediction: reflections on present status and challenges. *Faraday Discussions* **2018**, *211*, 643–660.

(25) Oganov, A. R.; Glass, C. W.; Lyakhov, A. O.; Zhu, Q.; Qian, G.; Stokes, H. T.; Bushlanov, P.; Allahyari, Z.; Graf, P.; Stevanovic, V. et al. Universal Structure Predictor: Evolutionary Xtallography. 2019.

(26) Oganov, A. R.; Pickard, C. J.; Zhu, Q.; Needs, R. J. Structure prediction drives materials discovery. *Nature Reviews Materials* **2019**, *4*, 331–348.

(27) Artacho, E.; Anglada, E.; Diéguez, O.; Gale, J. D.; García, A.; Junquera, J.; Martin, R. M.; Ordejón, P.; Pruneda, J. M.; Sánchez-Portal, D. et al. The SIESTA method; developments and applicability. *Journal of Physics: Condensed Matter* **2008**, *20*, 064208.

(28) Perdew, J. P.; Burke, K.; Ernzerhof, M. Generalized gradient approximation made simple. *Physical Review Letters* **1996**, *77*, 3865–3868.

(29) Giannozzi, P.; Baroni, S.; Bonini, N.; Calandra, M.; Car, R.; Cavazzoni, C.; Ceresoli, D.; Chiarotti, G. L.; Cococcioni, M.; Dabo, I. et al. Quantum ESPRESSO: a modular and open-source software project for quantum simulations of materials. *Journal of Physics: Condensed Matter* **2009**, *21*, 395502.

(30) Giannozzi, P.; Andreussi, O.; Brumme, T.; Bunau, O.; Nardelli, M. B.; Calandra, M.; Car, R.; Cavazzoni, C.; Ceresoli, D.; Cococcioni, M. et al. Advanced capabilities for materials modelling with Quantum ESPRESSO. *Journal of Physics: Condensed Matter* **2017**, *29*, 465901.

(31) Garrity, K. F.; Bennett, J. W.; Rabe, K. M.; Vanderbilt, D. Pseudopotentials for high-throughput DFT calculations. *Computational Materials Science* **2014**, *81*, 446–452.

(32) Baroni, S.; de Gironcoli, S.; Corso, A. D.; Giannozzi, P. Phonons and related crystal properties from density-functional perturbation theory. *Reviews of Modern Physics* **2001**, *73*, 515–562.

(33) Guo, Y.; Yu, C.; Lin, J.; Wang, C.; Ren, C.; Sun, B.; Huai, P.; Xie, R.; Ke, X.; Zhu, Z. et al. Pressure-induced structural transformations and polymerization in ThC_2. *Scientific Reports* **2017**, *7*, 2–11.

(34) Wagner, F. R.; Bende, D.; Grin, Y. Heteropolar bonding and a position-space representation of the 8 - N rule. *Dalton Trans.* **2016**, *45*, 3236–3243.

(35) Outeiral, C.; Vincent, M. A.; Martín Pendás, A.; Popelier, P. L. A. Revitalizing the concept of bond order through delocalization measures in real space. *Chem. Sci.* **2018**, *9*, 5517–5529.

(36) Montoya, J. A.; Hernandez, A. D.; Sanloup, C.; Gregoryanz, E.; Scandolo, S. OsN_2: Crystal structure and electronic properties. *Applied Physics Letters* **2007**, *90*, 011909.

(37) Birch, F. Finite Elastic Strain of Cubic Crystals. *Phys. Rev.* **1947**, *71*, 809–824.

(38) Wu, Z.-J.; Zhao, E.-J.; Xiang, H.-P.; Hao, X.-F.; Liu, X.-J.; Meng, J. Crystal structures and elastic properties of superhard IrN_2 and IrN_3 from first principles. *Phys. Rev. B* **2007**, *76*, 054115.

(39) Angel, R. J.; Alvaro, M.; Gonzalez-Platas, J. EosFit7c and a Fortran module (library) for equation of state calculations. *Zeitschrift für Kristallographie - Crystalline Materials* **01 May. 2014**, *229*, 405 – 419.

(40) Semenok, D. V.; Kruglov, I. A.; Savkin, I. A.; Kvashnin, A. G.; Oganov, A. R. On Distribution of Superconductivity in Metal Hydrides. *Current Opinion in Solid State and Materials Science* **2020**, *24*, 100808.

(41) Georges, A.; Kotliar, G.; Krauth, W.; Rozenberg, M. J. Dynamical mean-field theory of strongly correlated fermion systems and the limit of infinite dimensions. *Rev. Mod. Phys.* **1996**, *68*, 13–125.

Graphical TOC Entry